Advanced Steel Construction 2 (2006) 53-70

STEEL-CONCRETE COMPOSITE BEAMS PRESTRESSED BY EXTERNAL TENDONS: EFFECTS OF MATERIAL AND GEOMETRIC NONLINEARITIES

Andrea Dall'Asta[1,*], Laura Ragni[2] and Alessandro Zona[1]

[1] *Dipartimento di Progettazione e Costruzione dell'Ambiente, Università di Camerino*
Viale delle Rimembranza, 63100, Ascoli Piceno, Italy.
**(Corresponding author: E-mail: andrea.dallasta@unicam.it)*
[2] *Dipartimento di Architettura, Costruzioni e Strutture, Università Politecnica delle Marche*
Via Brecce Bianche 60131, Ancona, Italy.

Abstract: The analysis of externally post-tensioned beams is characterized by some specific issues related to the coupling between the local strain of the cable and the global deformation of the structure. Collapse modalities are influenced by the nonlinear behavior of materials and in many cases by non-negligible geometric nonlinear effects. The authors present a model for externally prestressed steel-concrete composite beams that includes geometric and material nonlinearities. The proposed model is based on the theory of small strains and moderate rotations obtained from the exact nonlinear theory. Comparisons with experimental tests are shown to validate the results obtained with the proposed formulation. Some numerical applications involving simply supported and two-span continuous composite beams post-tensioned with external cables are discussed to illustrate the nonlinear geometric effects and their influence on the ultimate capacity.

Keywords: External prestressing, steel-concrete composite beams, nonlinear analysis, material nonlinearity, geometric nonlinearity, finite elements.

1. INTRODUCTION

Externally prestressed steel-concrete composite members have been used since the late 1950s in buildings and bridge construction (e.g., Szilard [1], Hoadley [1]). External post-tensioning gives many advantages in new composite constructions, e.g., elastic behavior extended to higher loads, increased ultimate capacity, smaller deflections under service loads, reductions in beam depth and structural weight, control of deck cracking in continuous beams. These benefits may offset the extra costs of cables and deviators, and offer solutions of high aesthetic value. In addition external post-tensioning is extensively applied in existing bridges to reinforce damaged structures or to increase the ultimate capacity when larger than designed loads are applied (e.g., Berridge and Donovan [3], Mancarti [4]). Moreover, in new and old structures, it is possible to replace cables or to adjust their force whenever required.

The analysis of externally post-tensioned beams is characterized by a number of specific features. External tendons interact with the beam at anchorages and deviators only. Tendon-deviator relative slips are not prevented since negligible friction occurs in many common cases (e.g., Conti *et al.* [5]). Thus the local strain of the cable depends on the global deformation of the beam-tendon structural system. As a result a global analysis is required, where the balance conditions of the whole system replace the differential equations of the cross-section equilibrium.

At serviceability the displacements and strains of the beam-tendon system are small and the increment in tendon force can be neglected. In this case an approximate structural analysis can easily be performed by considering the effect of the cable on the beam as constant external equivalent loads and by carrying out a local linear analysis. At the ultimate state the prestressed system undergoes large deflections; as a consequence the cable traction increases and the beam-tendon relative position between two consecutive deviators changes considerably. Therefore geometric nonlinear effects as well as material nonlinearities cannot be neglected in a global analysis at collapse.

In the scientific literature there are a number of models including the nonlinear behavior of materials in the analysis of concrete or composite beams prestressed by external tendons. From simplified methods, such as Virlogeux [6], Saadatmanesh *et al.* [7], Ayyub *et al.* [8][9], to more general approaches considering different cable patterns and static schemes, such as Dall'Asta and Dezi [10]. The effects at collapse of geometric nonlinearities was included in few recent papers dealing with concrete beams only. From simplified iterative approaches where cable eccentricity is updated at each load step, such as Alkhairi and Naaman [11] and Harajli *et al.* [12], to more general models based on the finite element method where the cable position changes with respect to the beam when the system deflects (Ramos and Aparicio [13], Ariyawardena and Ghali [14]). These papers start from the geometric linear theory and then include the effect of the variation of the cable eccentricity that occurs when the beam deflects.

The aim of this work is to introduce a beam model for describing all the geometric nonlinear effects by means of a more rigorous method: the formulation for the beam-tendon system is deduced from the finite deformation theory (large displacements and finite strains). For this purpose a material and geometric nonlinear model within the finite deformation theory is first described, with reference to steel-concrete composite beams. The balance equations obtained are formally simple but their solution is quite complex. For simplifying the numerical solution, a reduced formulation based on the theory of small strains and moderate rotations (Naghdi and Vongsarnpigoon [15], Marzano and De Tommasi [16]) is afterward derived; hypotheses of small strain (up to 1/200) and moderate rotations (up to 1/20) are limitations compatible with the displacements observed at collapse in experimental tests. The weak form of the balance condition is obtained by considering the total Lagrangian formulation and the numerical solution is sought with a displacement-based finite element formulation (Dall'Asta and Zona [17]). The numerical model implemented is verified by comparison with experimental tests. Some numerical applications to simply supported and two-span continuous composite beams post-tensioned with external cables are reported to discuss the influence on the ultimate capacity of nonlinear geometric effects together with material nonlinearities affecting a reduction of stiffness and the redistribution of internal stress.

2. ANALYTICAL MODEL

2.1. Nonlinear Kinematics

The present formulation describes the behavior of a rectilinear beam prestressed by external tendons with generic path. Tendons are anchored at the beam ends and their profile is defined by a certain number of saddle points at which they can slip with negligible friction. The problem is assumed to be symmetric with respect to the vertical plane containing the beam axis. The analysis is carried out by assuming a Kirchhoff model for the beam deformation (i.e., the cross section remains plane and orthogonal to the beam axis after deformation) and no limits on amplitude of displacements and strain are assumed. Let $\{O: \mathbf{A}_i, i = 1, 2, 3\}$ be a fixed orthonormal basis, where $\mathbf{A}_3$ is parallel to the beam axis and $\mathbf{A}_1\mathbf{A}_3$ is the plane of symmetry of the system. The position of a generic point (X_1, X_2, S) of the beam in the reference configuration is given by

$$\mathbf{R}(X_\beta; S) = S\mathbf{A}_3 + X_\beta\mathbf{A}_\beta = \mathbf{R}_0 + X_\beta\mathbf{A}_\beta \qquad (\beta=1, 2) \tag{1}$$

where $(X_1, X_2) \in A$ and $S \in [0, L]$, being $A \subset R^2$ the domain of the cross section of the beam and L the beam length. A pair of external cables are considered and modeled as a unique tendon on the symmetry plane of the system. Its profile is described by the following piecewise linear function

$$\mathbf{H}(S) = \mathbf{H}_{d-1} + \frac{\mathbf{H}_d - \mathbf{H}_{d-1}}{|\mathbf{H}_d - \mathbf{H}_{d-1}|}(S - S_{d-1}) \qquad S \in [S_{d-1},\ S_d] \tag{2}$$

with $\mathbf{H}_d = \mathbf{R}_d$ where $\mathbf{R}_d = S_d\mathbf{A}_3 + X_{2d}\mathbf{A}_2$ (d = 1, ..., D) are the position of D beam points where

the deviators and end anchorages are located (Figure 1). The total length of the tendon is

$$L_t = \sum_d \left|\mathbf{R}_d - \mathbf{R}_{d-1}\right| = \sum_d \sqrt{\left[\Delta_d(S)\right]^2 + \left[\Delta_d(X_2)\right]^2} \tag{3}$$

The beam and the tendon are two different geometric entities that constrain each other, so that the system deformation is described by two coupled functions.

The deformed configuration of the beam, where the cross sections do not deform transversally, can be described by the following function (Simo [18], Simo and Vu-Quoc [19])

$$\mathbf{r}(X_\beta; S) = \mathbf{r}_0(S) + X_\beta \mathbf{Q}(S)\mathbf{A}_\beta \tag{4}$$

where $\mathbf{r}_0(S)$ describes the deformed position of the beam axis and $\mathbf{Q}$ is the rotation matrix

$$\mathbf{Q}(S) = \mathbf{I} + \sin\alpha(S)\boldsymbol{\Omega} + \left[1 - \cos\alpha(S)\right]\boldsymbol{\Omega}^2 \tag{5}$$

that describes the section rotations ($\mathbf{I}$ is the identity operator and $\boldsymbol{\Omega} = \mathbf{A}_2 \otimes \mathbf{A}_3 - \mathbf{A}_3 \otimes \mathbf{A}_2$). Consequently the displacements are

$$\mathbf{u}(X_\beta; S) = \left[v(S) - X_2(1-\cos\alpha)\right]\mathbf{A}_2 + \left[w(S) - X_2(1-\sin\alpha)\right]\mathbf{A}_3 \tag{6}$$

where $v(S)$ and $w(S)$ are two scalar functions expressing the displacements of the beam axis in directions $\mathbf{A}_2$ and $\mathbf{A}_3$ respectively. From the assumption of orthogonality between cross sections and beam axis, the rotation is a function of the displacements

$$\sin\alpha = \frac{v'}{1+e} \qquad\qquad \cos\alpha = \frac{1+w'}{1+e} \tag{7a,b}$$

where the prime denotes the derivative with respect to S and $e = \sqrt{v'^2 + (1+w')^2} - 1$. Let $\mathbf{F}$ be the deformation gradient (Malvern [20])

$$\mathbf{F} = \mathbf{QU} = \mathbf{Q}\left[(e + \alpha' X_2)\mathbf{A}_3 \otimes \mathbf{A}_3 + \mathbf{I}\right] = \mathbf{Q}\left[\varepsilon \mathbf{A}_3 \otimes \mathbf{A}_3 + \mathbf{I}\right] \tag{8}$$

where $\mathbf{U}$ is the deformation tensor and ε the beam axial deformation. It is worth noting that the axial deformation ε is the only non zero strain component.

The cable profile in the deformed configuration can be described by means of a piecewise linear function

$$\mathbf{h}(S) = \mathbf{h}_{d-1} + \frac{\mathbf{h}_d - \mathbf{h}_{d-1}}{\left|\mathbf{h}_d - \mathbf{h}_{d-1}\right|}(S - S_{d-1}) \qquad\qquad S \in [S_{d-1},\ S_d] \tag{9}$$

that is connected to the beam at the saddle points $\mathbf{h}_d = \mathbf{r}_d$ (i.e. anchorages and deviators). Because of the cable slip there is no correspondence between the material points at the position $\mathbf{H}(S)$ in the reference configuration and the material points at the position $\mathbf{h}(S)$ in the deformed configuration (Dall'Asta [21]). For this reason it is not trivial to deduce the deformed cable position. Nevertheless by assuming that the friction at the deviators is negligible the cable deformation is uniform and can be deduced from the total profile length only without quantifying the tendon slip at each deviator

$$\varepsilon_t = \frac{1}{L_t}\sum_d \left(\left|\mathbf{r}_d - \mathbf{r}_{d-1}\right| - \left|\mathbf{R}_d - \mathbf{R}_{d-1}\right|\right) \tag{10}$$

where

$$l_t = \sum_d \left|\mathbf{r}_d - \mathbf{r}_{d-1}\right| = \sum_d \sqrt{\left[\Delta_d(S) + \Delta_d(w) - \Delta_d(X_2 \sin\alpha)\right]^2 + \left[\Delta_d(v) + \Delta_d(X_2\cos\alpha)\right]^2} \tag{11}$$

with l_t the cable length in the deformed configuration and $\Delta_d(\bullet) = (\bullet)_d - (\bullet)_{d-1}$.

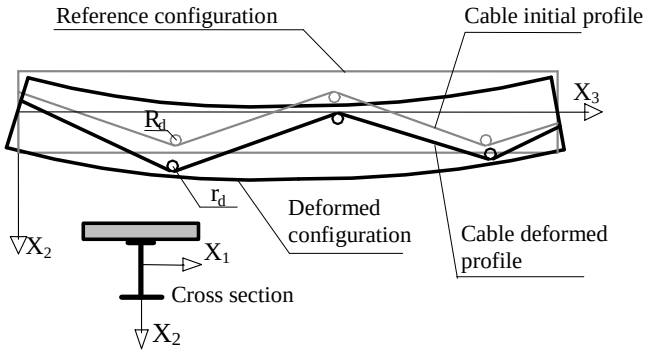

Figure 1. Beam with external prestressing

2.2. Moderate Rotations Formulation

The beam-tendon model previously illustrated is able to describe large deformations of the system without limitations on the displacement field. It is however rather complicated to obtain a numerical solution of the problem. In addition it can be observed that the collapse of beams usually used in bridge structures occurs when the maximum strains of materials are very small and attain values from about 0.2 % to 1.0 %, while the maximum rotations of the cross sections are about 1/20 that can be considered as a moderately small quantity. This makes it convenient to develop a simplified theory, able to describe real situations, by introducing some hypotheses on the displacement field. The aim of this paragraph is to develop an approximated nonlinear theory by considering the hypothesis that the symmetric and anti-symmetric parts of the displacement gradient have a different magnitude

$$\mathbf{E} = \frac{1}{2}\left(\nabla\mathbf{u} + \nabla\mathbf{u}^{\mathrm{T}}\right) = \mathrm{O}(\eta) \qquad \text{and} \qquad \mathbf{W} = \frac{1}{2}\left(\nabla\mathbf{u} - \nabla\mathbf{u}^{\mathrm{T}}\right) = \mathrm{O}\left(\eta^{1/2}\right) \tag{12a,b}$$

where η is a measure of smallness (Naghdi and Vongsarnpigoon [15]). Consequently the deformation tensor **U** and the rotations tensor **Q** can be approximated as

$$\mathbf{U} = \mathbf{I} + \mathbf{E} - \frac{1}{2}\mathbf{W}^2 + \mathrm{o}(\eta) \tag{13}$$

$$\mathbf{Q} = \mathbf{I} + \mathbf{W} + \frac{1}{2}\mathbf{W}^2 + \mathrm{o}(\eta) \tag{14}$$

In other words $\mathbf{U} - \mathbf{I} = \mathrm{O}(\eta)$ and $\mathbf{Q} - \mathbf{I} = \mathrm{O}\left(\eta^{1/2}\right)$. This means that a local deformation is given by a small strain and a moderate rotation (Marzano and De Tommasi [16]).
With reference to the described beam model, assumption (12b) leads to the following formulas

$$\sin\alpha = v' + \mathrm{o}(\eta) \qquad \cos\alpha = 1 - \frac{1}{2}v'^2 + \mathrm{o}(\eta) \tag{15a, b}$$

and the displacement field becomes

$$\mathbf{u} = \left(v - \frac{1}{2}X_2 v'^2\right)\mathbf{A}_2 + \left(w - X_2 v'\right)\mathbf{A}_3 + \mathrm{o}(\eta) \tag{16}$$

while the strain of a generic fiber measured in its deformed configuration is given by

$$\varepsilon = w' + \frac{1}{2}v'^2 - X_2 v'' + \mathrm{o}(\eta) \tag{17}$$

The difference with respect to the linear theory consists of the quadratic term that represents the axial strain of a generic fiber due to its rotation that can be added to the strain due to its axial deformability. Hence the vertical displacements of the beam influence its axial strain and this may be interpreted as a reduction of the beam axial stiffness caused by its deflection.

It is important to remark that limitations not only on the beam displacements but also on the beam

geometry are necessary to obtain expression Eq. (16). In particular the following hypotheses are required

1. $w' = \mathrm{O}(\eta)$;
2. $Lv'' = \mathrm{O}(\eta^{1/2})$;
3. $X_2 / L = \mathrm{O}(\eta^{1/2})$.

From the second hypothesis derives $v' = \mathrm{O}(\eta^{1/2})$ and $v'^2 = \mathrm{O}(\eta)$ being $v' = \int_0^L v'' dz \le L \sup(v'')$.

The last hypothesis on beam slenderness is necessary in Eq. (17) if the deformations are to remain small despite the fact that rotations are moderate. It is important to note that this hypothesis is acceptable in the cases in question. In fact, with reference to the beams used in bridge construction, depth-to-span ratios are about equal to 1/20 which can be considered as moderately small quantities.

While the beam problem is already known, the extension of the small strains and moderate rotations theory to the cable terms needs further consideration. The simplified expression of the cable deformation measured in its deformed configuration is given by

$$\varepsilon_t = \frac{1}{L_t}\left\{\sum_d \left[\Delta_d(S) + \Delta_d(w) + \frac{1}{2}\frac{[\Delta_d(X_2) + \Delta_d(v)]^2}{\Delta_d(S)} - \Delta_d(X_2 v')\right] - L_t\right\} + \mathrm{o}(\eta) \qquad (18)$$

where L_t is the tendon length in the reference configuration and can be written as

$$L_t = \Delta_d(S) + \frac{[\Delta_d(X_2)]^2}{2} + \mathrm{o}(\eta) \qquad (19)$$

A geometric hypothesis, similar to the third hypothesis is also necessary for the cable. In particular the strain ε_t remains small if the inclination of the cable profile is moderate, in the following sense

4. $\dfrac{\Delta_d(X_2)}{\Delta_d(S)} = \mathrm{O}(\eta^{1/2})$

This hypothesis is realistic if the cable pattern is included in the beam depth, as in most cases. Also for the cable the difference between this theory and the linear theory (Dall'Asta and Dezi [10]) consists of a quadratic term. In this case the quadratic contribution does not involve the vertical displacements only, but depends on the initial cable inclination by means of the mixed term $\Delta_d(X_2)\Delta_d(v)$. Consequently this deformation becomes more important when the cable initial inclination increases.

Because of the particular compatibility condition in which the cable strain depends on the displacements of all the saddle points, it is not convenient to write the balance condition in terms of equilibrium of the beam cross sections (local equilibrium). A global balance condition of the whole system can be deduced by starting from the general expression of the virtual work theorem

$$\int_V \sigma\hat{\varepsilon} dV + L_t A_t \sigma_t \hat{\varepsilon}_t = \int_{[0,L]} \mathbf{t}_0 \cdot \hat{\mathbf{u}}_0 dS + \mathbf{T}_{0\theta} \cdot \hat{\mathbf{u}}_{0\theta}\big|_{\theta=0,L} \qquad \forall \hat{\varepsilon}, \hat{\varepsilon}_t, \hat{\mathbf{u}}_0 \subset U \qquad (20)$$

where $\mathbf{t}_0$ and $\mathbf{T}_0$ are the forces related to the beam axis line and beam ends respectively and U is the space of displacements and strains compatible with internal and external constraints. It should be observed that beam-tendon interaction terms do not appear in this equation because of the no friction assumption. In the following expression the two functions v(S) and w(S) which furnish the displacement field **u** are assumed as the problem unknowns and generic nonlinear constitutive laws are introduced for the tendon and the beam

$$\sigma = \sigma(\varepsilon) \tag{21}$$

$$\sigma_t = \sigma_t(\varepsilon_t - \varepsilon_{t0}) \tag{22}$$

where σ is the normal stress of a generic beam fibre and σ_t is the tendon stress. The configuration in which the beam is in its natural state (zero stress) is chosen as the reference configuration. In this configuration the stress σ_t in the cable is not null and can be controlled by the initial cable strain ε_{t0}. The virtual strains, according to the moderate rotation theory, have the following expressions

$$\hat{\varepsilon} = \hat{e} + X_2\hat{\alpha}' = v'\hat{v}' + \hat{w}' - X_2\hat{v}'' \tag{23}$$

$$\hat{\varepsilon}_t = \frac{1}{L_t}\sum_d \left[\mathbf{g}_d \cdot \Delta_d(\hat{\mathbf{u}})\right] = \frac{1}{L_t}\sum_d \left[\left(\Delta_d(\hat{w}) + \frac{\Delta_d(X_2) + \Delta_d(v)}{\Delta_d(S)}\Delta_d(\hat{v}) - \Delta_d(X_2\hat{v}')\right)\right] \tag{24}$$

where $\mathbf{g}_d$ is the unit vector in the direction of the tract considered after its deformation (Dall'Asta [21]). Consequently the following expression is obtained

$$\begin{aligned} &\int_{[0,L]} \left(N\hat{w}' + Nv'\hat{v}' + M\hat{v}''\right)dS + \\ &+ t_t \sum_d \left(\Delta_d(\hat{w}) + \frac{\left(\Delta_d(X_2) + \Delta_d(v)\right)}{\Delta_d(S)}\Delta_d(\hat{v}) - \Delta_d(X_2\hat{v}')\right) = \qquad \forall \hat{v}, \hat{w} \in U \\ &= \int_{[0,L]} \left(t_{02}\hat{v} + t_{03}\hat{w}\right)dS + \left(T_{02\theta}\hat{v}_\theta + T_{03\theta}\hat{w}_\theta\right)\Big|_{\theta=0,L} \end{aligned} \tag{25}$$

where t_{02} and t_{03} represent the transversal and longitudinal forces acting on the beam, while T_{02} and T_{03} are the total forces acting on the beam ends along the longitudinal and transverse directions respectively, while N, M, t_t are the total force and total moment at beam cross sections and the total tendon force respectively, given by the following expressions

$$N = \int_\Omega \sigma d\mathbf{X} \tag{26}$$

$$M = -\int_\Omega \sigma X_2 d\mathbf{X} \tag{27}$$

$$t_t = A_t\sigma_t \tag{28}$$

where Ω is the cross section domain. Eq. (25) is a global balance condition where the equilibrium of the whole system is enforced in the deformed configuration. This formulation (i.e., Lagrangian formulation) is very convenient since each quantity (e.g., length, surface, volume etc.) is referred to the known reference configuration.

3. NUMERICAL SOLUTION

3.1. Nonlinear finite element model

The solution of the geometric and material nonlinear problem defined by Eq. (25) is obtained with the finite element method. The numerical code implemented is based on the approach described in (Dall'Asta and Zona [17]) where the geometric linear formulas are substituted by the relevant formulas of the moderate rotations theory.

A 10 degrees-of-freedom (DOF) beam element is adopted, i.e., two end nodes each with three DOF (axial displacement, transverse displacement, rotation) and four intermediate nodes with one axial DOF. Shape functions are third-order Hermite polynomials for transverse displacement v(S) and fifth-order polynomials for axial displacement w(S). Using these shape functions any inconsistency between axial and flexural displacement fields is avoided as can be demonstrated with considerations similar to those presented in (Dall'Asta and Zona [22]). The numerical integrations at the cross-section level are performed by subdividing the domain into a number of fibers parallel

to the X_3 axis. The numerical integrations along the beam axis are performed by using the Gauss rule with 7 points. External prestressing cables are included in the finite element model by assuming that the positions of deviators and end anchorages coincide with some of the nodal points of the finite element subdivision. Thus the cable deformation is a function of the nodal displacement vector of the structure, as described in (Dall'Asta and Zona [17]) for the geometric linear case.

The strategies adopted for the solution of the resulting nonlinear problem are the tangent Newton-Raphson iterative procedure combined with load control and displacement incremental procedures. The load control procedure is used for the first steps of the nonlinear analysis (i.e., the initial stiffness is not reduced by degradation of materials), while displacement control is used for tracing the nonlinear path up to collapse (i.e., reduced stiffness giving small load variations along with large deflection increments or even softening branches).

3.2. Material constitutive laws

General nonlinear constitutive material models can be implemented in the finite element formulation based on the proposed approach. In the numerical applications illustrated in this work the following material constitutive laws are adopted.

The concrete in compression is modeled by using the CEB-FIP Model Code 90 [23]; a linear law up to tensile strength, followed by descending exponential law is used for the concrete in traction (Figure 2a). Since the concrete constitutive law has a softening branch after the strength peak, mesh-sensitive results may be obtained. This problem can be overcome if the minimum admissible element size is specified; its suitable value is equal to the beam depth (Bazant *et al.* [24]).

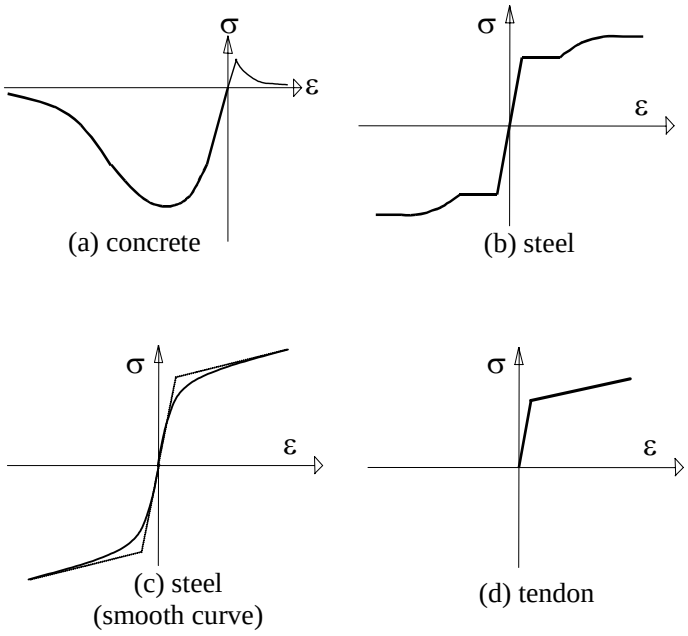

Figure 2. Constitutive laws

The steel material (either steel for reinforcements and beam steel) is modeled by using an elastic - perfect plastic - hardening law (Bruneau *et al.* [25]). The elastic - perfect plastic branches are given by linear functions while the hardening tract is an exponential function (Figure 2b). This constitutive model is characterized by a sharp transition from the elastic to the plastic range. In common cases however, due to residual stresses in the steel beam section, the resulting behavior of the beam shows a gradual shift from the elastic to the plastic range. To model these cases a second steel constitutive law is included, i.e., the uniaxial Menegotto-Pinto [26] constitutive model, a smooth curved transition from an asymptotic straight line with slope E_0 to another asymptotic straight line with slope E_1 (Figure 2c). The Menegotto-Pinto equation, originally proposed for reinforcing bars, is a computationally efficient nonlinear smooth model for structural steel permitting very good agreement with experimental results (Bruneau *et al.* [25]).

The tendon steel behavior is described by a bilinear elastic - hardening law (Figure 2d).

The constitutive laws for steel beam, steel reinforcements and prestressing cable are characterized

by assigned ultimate strains; zero stiffness and zero stress are assumed beyond these ultimate strains. The collapse of the structure in the finite element nonlinear analysis is attained when the ultimate strain in the steel (beam, reinforcements or tendon) is reached. In some cases, however, the collapse condition might be determined by the crushing of concrete. In fact exceeding the concrete peak strain might lead to a tangent stiffness matrix of the structure that becomes singular due to the negative stiffness contributions given by the softening branch.

4. COMPARISONS WITH EXPERIMENTAL TESTS

A limited number of experimental tests on steel-concrete composite beams prestressed by external tendons are available in literature. In some of these tests the geometric nonlinearity does not significantly influence the structural behavior due to the reduced beam slenderness. This is the case of the tests previously used for validating the geometric linear model (Dall'Asta and Zona [17]), capable in these conditions of giving results in very good agreement with the experimental tests. In a few situations however the beam geometry and the cable path are such as to highlight the effects of the geometric nonlinearity. This is for example the case of recent tests published by Chen and Gu [27] and used for validation purposes in this work. A comparison with the results of the simply supported beam tested is discussed hereafter. The beam, indicated as BS2 in (Chen and Gu [27]), is prestressed by a rectilinear eccentric cable without intermediate deviators and is subject to two-point symmetric loading. For details on the geometric and material properties the reader may refer to (Chen and Gu [27]).

The beam was unevenly subdivided in eight beam elements and the analysis was carried out in three phases: I) beam without prestressing under self-weight load (load control analysis); II) jacking of the prestressing tendons under self-weight load up to the initial experimental cable traction (load control analysis with null increase of the applied loads); III) application of the two-point symmetric loading on the beam and increase of these two forces up to collapse (displacement control analysis with mid span deflection as controlled degree-of-freedom). The Menegotto-Pinto constitutive model was preferred over the elastic – plastic – hardening law for the steel beam for a more accurate description of the structural response in the transition phase between linear and plastic ranges.

In Figures 3 and 4 the numerical results (lines) and the experimental measures (series of points) are compared. The numerical results are obtained by the moderate rotation geometric nonlinear model illustrated in this work and by the correspondent material-nonlinear-only model. Good agreement

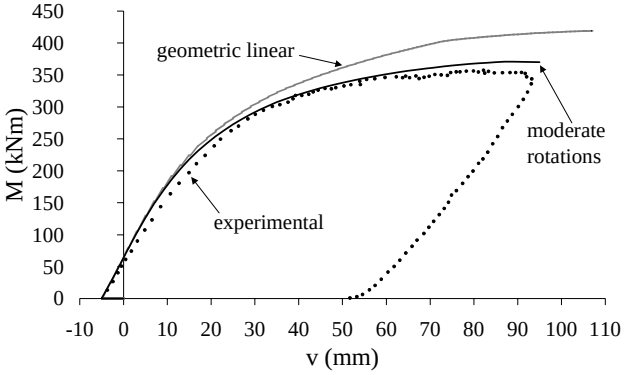

Figure 3. Comparison with experimental test: moment – mid span deflection curves for beam BS2

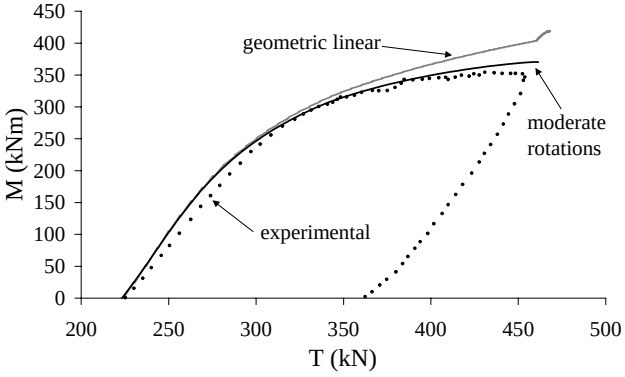

Figure 4. Comparison with experimental test: moment – cable traction curves for beam BS2

between the moderate rotation model and the experimental results is attained, both in the bending moment versus mid span deflection curve and in the bending moment versus cable traction curve. The geometric linear model overestimates the ultimate capacity of the beam due to the importance of geometric nonlinearity affecting the beam structural behavior.

5. NUMERICAL APPLICATIONS

The geometric nonlinear effects and the difference between the moderate rotation model and the geometric linear model are thoroughly investigated and discussed in this section by means of numerical applications to slender steel-concrete composite beams with different structural configurations (simply supported and continuous beams) and different cable profiles. Each beam has equal steel concrete composite section (Figure 5), span length (L = 46 m) and thus span-to-depth ratio (L/h = 28.75), total area of the prestressing tendons (A_{tot} = 10000 mm^2), and material properties (Table 1). The beam cross section was designed to prevent local buckling phenomena of the web and overall instabilities under the applied loads and prestressing. The nonlinear analysis was divided into three phases: I) application of a uniform load q_1 = 30 kN/m representative of the structural self-weight on the non prestressed beam; II) jacking of the tendons to the total initial prestressing force T_0 = 11400 kN; III) application of a distributed uniform load q_2 that is increased through to collapse. In the first two phases the nonlinear analysis was carried out

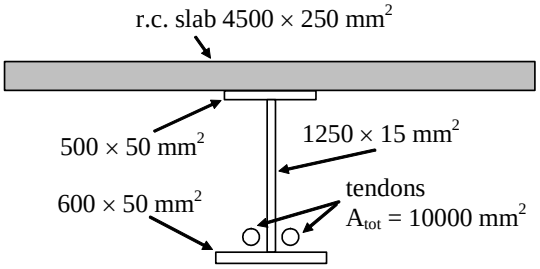

Figure 5. Cross section of the beams tested

Table 1. Material parameters

	Concrete (compression)	Concrete (tension)	Reinforcement steel	Beam steel	Tendon
Yielding stress	-	-	f_y = 430 MPa	f_y = 275 MPa	f_y = 1600 MPa
Strength	f_c = 33 MPa	f_{ct} = 2.50 MPa	f_t = 473 MPa	f_t = 360 MPa	f_t = 1800 MPa
Elastic modulus	E_{ci} = 32000 MPa	E_{ct} = 30500 MPa	E_s = 200 GPa	E_s = 200 GPa	E_s = 200 GPa
Hardening strain	-	-	ε_h = 0.02	ε_h = 0.04	-
Ultimate strain	-	-	ε_u = 0.12	ε_u = 0.18	ε_u = 0.10

by using the load control procedure, the third phase by using the displacement control method with mid span deflection of the loaded span as controlled degree-of-freedom. The beams were unevenly subdivided in 24 elements per span. Each beam was analyzed by using the proposed geometric nonlinear model and the results are compared to those computed with a geometric linear model previously presented (Dall'Asta and Dezi [10]) and implemented in the finite element framework (Dall'Asta and Zona [17]) now extended to the moderate rotations model.

5.1. Simply supported beams with rectilinear tendon path

Three simply supported beams with rectilinear cable path are analyzed: beam R0 with no intermediate deviators, beam R1 with one deviator, and beam R2 with two deviators (Figure 6). The relevant load-deflection curves are reported in Figure 7. Values of the peak load $q_{max} = q_1 + \lambda_{max} q_2$ with the corresponding mid span deflection v_{max} and values of the ultimate mid

span deflection v_{ult} and the corresponding load $q_{ult} = q_1 + \lambda_{ult} q_2$ are given in Table 2 for each beam and analysis type. Results for the non prestressed (NP) case is also included in Table 2. The geometric nonlinear analysis shows significant differences of behavior between the three cable paths. One intermediate deviator permits an increase of 23.2% of the peak load with respect to the solution without intermediate deviators. Two intermediate deviators are less efficient and the increase of the peak load is 14.5%. Even larger is the increase of deflection associated to the load peak (increment of ductility). On the other hand the geometric linear analysis cannot describe the behavior differences due to deviators because only the displacement component parallel to the initial cable profile is measured (Dall'Asta and Dezi [10]). Thus one curve is representative for the three beams R0, R1, and R2 when a geometric linear analysis is performed. In this case the peak load level is overestimated with respect to the geometric nonlinear analysis of 25.2%, 1.7%, and 9.5% for beams R0, R1 and R2 respectively.

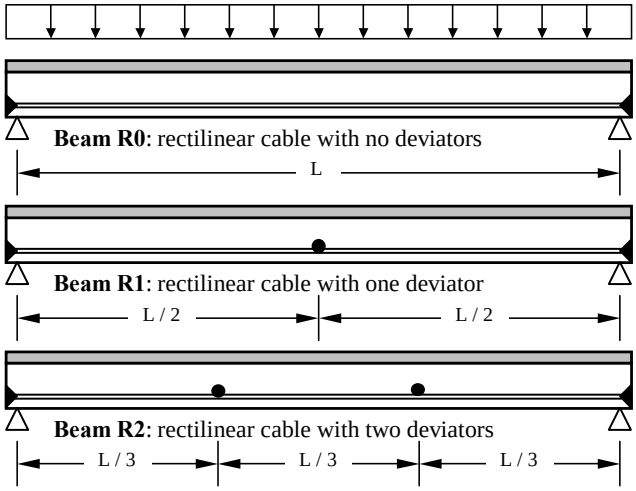

Figure 6. Beams with rectilinear tendon tested

Table 2. Simply supported beams tested: loads and mid span deflections

Beam	Moderate rotations analysis				Geometric linear analysis			
	q_{max}	$v(q_{max})$	q_{ult}	v_{ult}	q_{max}	$v(q_{max})$	q_{ult}	v_{ult}
	(kN/m)	(mm)	(kN/m)	(mm)	(kN/m)	(mm)	(kN/m)	(mm)
NP	73.20	1635	73.20	1635	73.20	1635	73.20	1635
R0	113.64	324	99.28	764	142.33	871	142.33	871
R1	139.95	1034	139.95	1034				
R2	130.16	699	130.04	729				
D1	125.99	892	125.73	962	144.76	1222	144.76	1222
D2	137.56	748	137.56	748	151.07	872	151.07	872

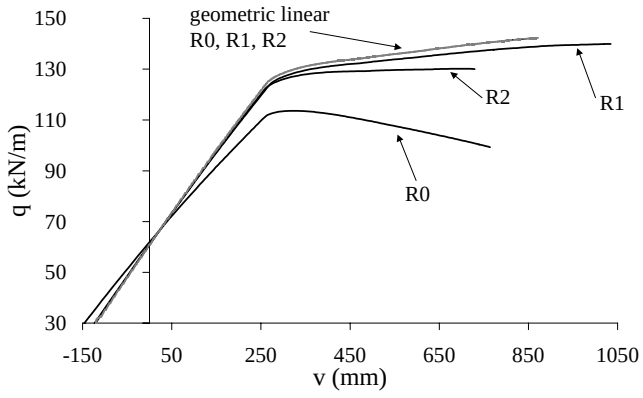

Figure 7. Beams R0, R1, and R2: load – mid span deflection

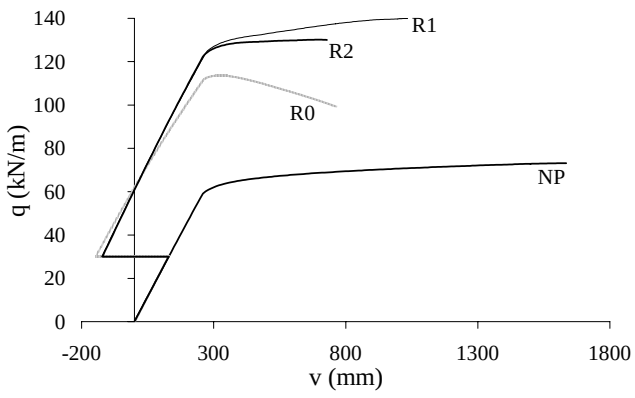

Figure 8. Beams R0, R1, R2 and NP: load – mid span deflection (moderate rotation analysis)

Comparing the results for the prestressed beams with the results of the non prestressed beam (Table 2 and Figure 8), significant increases are observed in the carrying load capacity (55% for R0, 91% for R1, 78% for R2 from the moderate rotations analysis) as well as a significant decrease of the ultimate deflection. It can also be noticed that the moderate rotations analysis and the material-nonlinear-only analysis give the same results for the non prestressed beam.

Figure 9 shows that in beam R0 under the same deflection level the tendon force is smaller when moderate rotation analysis is performed (the cable traction is represented in non-dimensional units by dividing its value T by the value of the initial traction T_0). The geometric linear formulation in fact includes only the stress variations due to axial deformations and end rotations, conversely the moderate rotation theory also includes the stress variation deriving from the beam ends coming up to each other due to vertical deflection of the beam. In beams R1 and R2 the tendon traction is larger than in beam R0; in beam R1 it is even higher than the value obtained by geometric linear analysis. In fact when the cable is rectilinear, the geometric linear analysis is not able to consider the elongation caused by the vertical displacements of deviators. This contribution becomes remarkable after beam yielding.

A larger prestressing force under the same load level is obtained from the geometric nonlinear analysis in beams R0, R1, R2 (Figure 10) because of the major deflections of the beam as computed including the geometric nonlinearity.

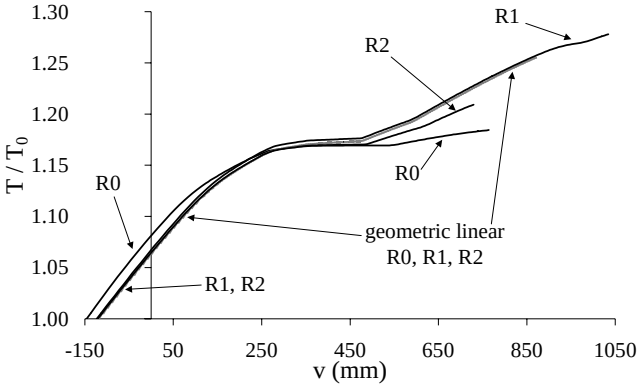

Figure 9. Beams R0, R1, and R2: cable traction – mid span deflection

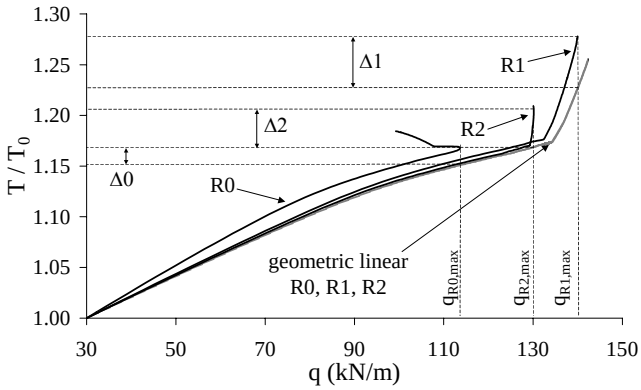

Figure 10. Beams R0, R1, and R2: cable traction – load.

In Figure 11 the total bending moment and the bending moment due to prestressing force only are plotted for each beam under the corresponding peak load level (i.e., $q_{R0,max}$ for R0, $q_{R1,max}$ for R1, and $q_{R2,max}$ for R2). The bending moment is represented in non-dimensional units by dividing its value by the positive plastic moment of the composite cross-section (M_{pl} = 19256.29 kNm). The bending moments computed by the geometric linear analysis under the same load levels are also plotted. It is observed that at anchorages and deviators the negative bending moment due to prestressing only has a larger absolute value in the geometric nonlinear analysis than in the geometric linear analysis. This can be explained by considering the larger prestressing force under the same load level (Figure 10). The amount of these bending moment differences are proportional to the difference of the external prestressing force highlighted in Figure 10. Conversely in sections sufficiently far from anchorages and deviators the absolute value of the negative bending moment due to external prestressing is smaller in the geometric nonlinear analysis than in the geometric linear analysis. The reason is in the cable eccentricity variation (included in the nonlinear geometric analysis but not in the geometric linear analysis) that has a stronger effect than the higher tendon traction. As a result the total bending moment (summation of the negative bending moment due to prestressing and of the positive bending moment due to external loads) is larger in the geometric nonlinear analysis in sections sufficiently far from deviators and anchorages.

In beam R0 the difference in bending moment due to prestressing between geometric linear and nonlinear analyses is remarkable. This significant variation of bending moment in the critical sections leads to the differences in ultimate load and ductility of the system. In beam R1 the presence of intermediate deviators makes it possible to increase the ultimate load and ductility and to reduce the differences between the geometric linear and nonlinear analysis. Furthermore, in this case the sections where the maximum bending moment is attained are different in the two analyses. The behavior of beam R2 is similar to that in beam R0 but the two intermediate deviators strongly reduce the differences between the two analysis. This means that the efficiency of deviators depends not only on their number but also on their position along the beams. In particular a deviator located at the critical section of the non prestressed beam strongly reduces the geometric nonlinear effects that decrease the ultimate capacity and ductility of the beam-cable system.

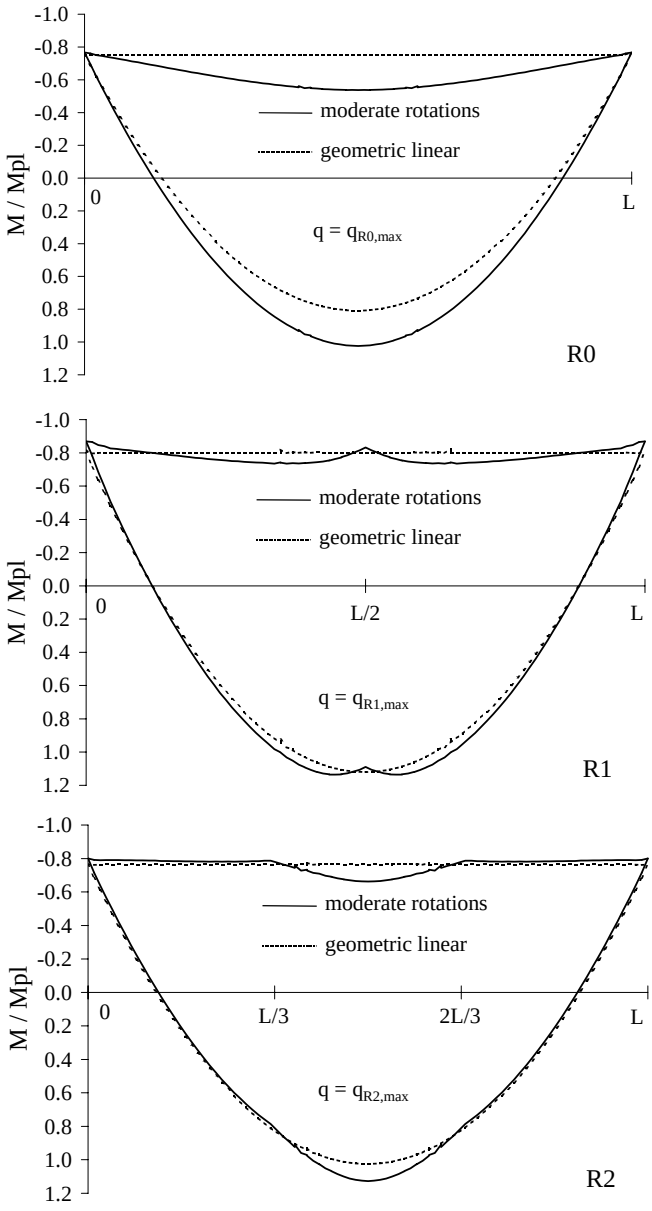

Figure 11. Total bending moment and moment due to prestressing force for beams R0, R1, and R2

5.2. Simply supported beams with draped tendon path

Two simply supported beams with draped cable path are analyzed: beam D1 and beam D2 with one and two intermediate deviators respectively (Figure 12). The relevant load-deflection curves are reported in Figure 13. Values of the peak load q_{max} with the corresponding mid span deflection v_{max} and values of the ultimate mid span deflection v_{ult} and the corresponding load q_{ult} are given in Table 2.

The geometric nonlinear analysis shows that prestressing with draped cables increases the load carrying capacity of the non prestressed beam (NP) of 72% and 88% when using one and two intermediate deviators respectively. The increase of the strength is associated to a significant reduction of deflections (Table 2 and Figure 14).

When draped tendons are used the geometric linear analysis can describe the behavior differences due to deviators. Both analyses

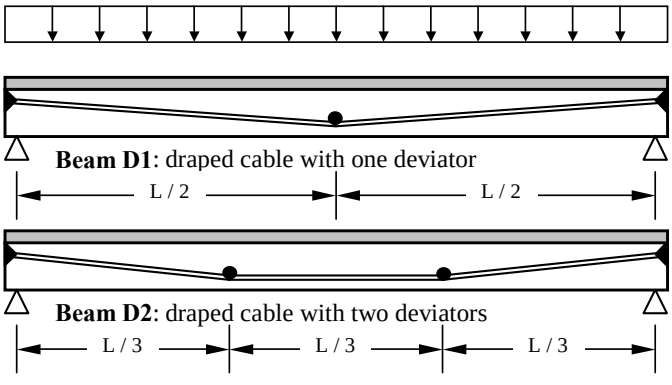

Figure 12. Simply supported beams with draped tendon tested

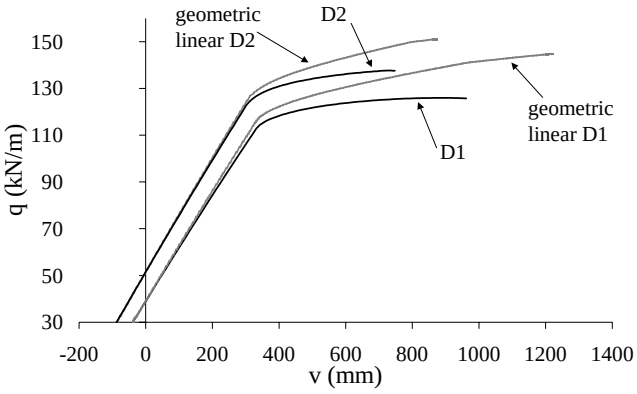

Figure 13. Beams D1 and D2: load – mid span deflection

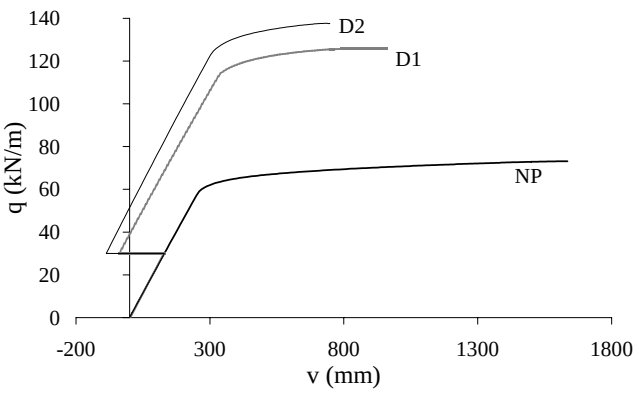

Figure 14. Beams D1, D2, and NP: load – mid span deflection (moderate rotations analysis)

can in fact consider the elongation due to vertical displacements of deviators although the geometric linear analysis does not consider the influence of the initial inclination of the cable profile tract. The peak load level is overestimated with respect to the geometric nonlinear analysis of 14.8%, and 9.8% for beams D1 and D2 respectively while the overestimation of the ultimate deflection is larger (Table 2).

In Figure 15 it is observed that tendon forces at the same deflection level is smaller in the moderate rotation analysis. Both geometric linear and nonlinear analyses include the contribution of vertical displacement of deviators, even if evaluated in a different way. The reduction in tendon force due to the beam ends coming up to each other because of the vertical deflection of the beam also occurs, as already mentioned in the previous case of rectilinear tendon. On the other hand larger prestressing forces under the same load level obtained from the geometric nonlinear analysis (Figure 16) are due to the major deflections of the beam as computed including the geometric nonlinearity.

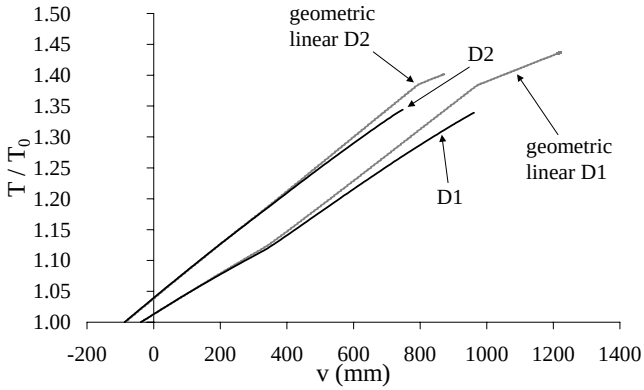

Figure 15. Beams D1 and D2: cable traction – mid span deflection

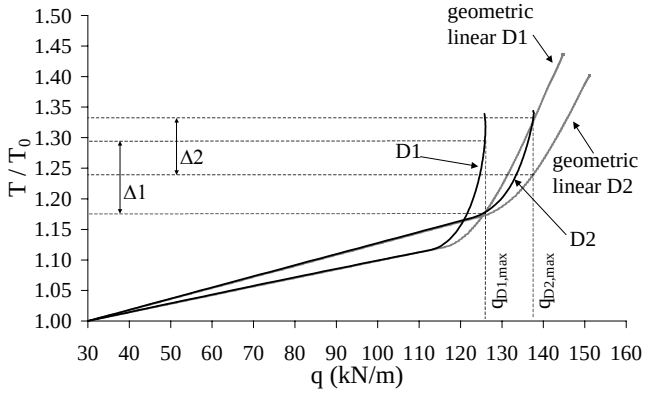

Figure 16. Beams D1 and D2: cable traction – load.

In Figure 17 the total bending moment and the bending moment due only to prestressing force are plotted for each beam under the corresponding peak load level (i.e., $q_{D1,max}$ for D1, and $q_{D2,max}$ for D2). The bending moments computed by the geometric linear analysis under the same load levels are also plotted. It is observed that at intermediate deviators the negative bending moment due to prestressing only has a larger absolute value in the geometric nonlinear analysis than in the geometric linear analysis. The reason is in the larger prestressing force under the same load level. The amount of these bending moment differences are proportional to the difference of external prestressing force highlighted in Figure 16. Conversely in sections sufficiently far from deviators the absolute value of the negative bending moment due to external prestressing is smaller in

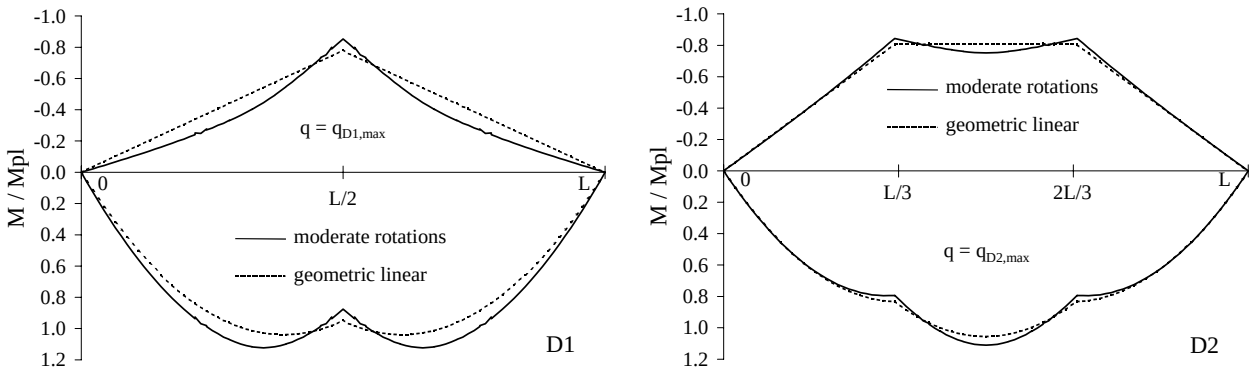

Figure 17. Total bending moment and moment due to prestressing force for beams D1 and D2

geometric nonlinear analysis than in geometric linear analysis. Cable eccentricity variation in fact has a stronger effect that the higher tendon traction, as in the previous case of rectilinear tendons. Accordingly the total bending moment is larger in the geometric nonlinear analysis in sections sufficiently far from deviators. In the critical sections the significant variation of bending moment leads to the differences in ultimate load and ductility of the system.

5.3. Two-span continuous beam with draped tendon path

A continuous beam with two equal spans of length L = 46 m and with cable path defined by three intermediate deviators is analyzed (Figure 18). Symmetric (CD3S) and non symmetric (CD3N) load patterns are considered. In phase I (only self-weight) and phase II (jacking under self-weight load) the symmetric uniform load q_1 representing self-weight is applied along the two spans and kept constant in both beams CD3S and CD3N. In phase III the uniform load q_2 is applied and increased in both spans in the symmetric load case (CD3S) while q_2 is applied and increased in the first span only in the non symmetric load case (CD3N). The relevant load-deflection curves are reported in Figure 19. A three-stage behavior of the beam is observed under symmetric loading (i.e., uncracked state, cracked state, plastic state) while the same beam under non symmetric loading is in cracked state right from the first steps of the analysis and the resulting behavior is subdivided in two stages (i.e., cracked state, plastic state). Values of the peak load $q_{max} = q_1 + \lambda_{max} q_2$ with the corresponding mid span deflection v_{max} and values of the ultimate mid span deflection v_{ult} and the corresponding load $q_{ult} = q_1 + \lambda_{ult} q_2$ in the first span are given in Table 3 for each load case and analysis type. Results for the non prestressed case are also included (CNPS and CNPN for the symmetric and non symmetric case respectively). The geometric nonlinear analysis shows that prestressing in the continuous beam considered increases the load carrying capacity 54% and 46% under symmetric and non symmetric loading respectively. Once again the

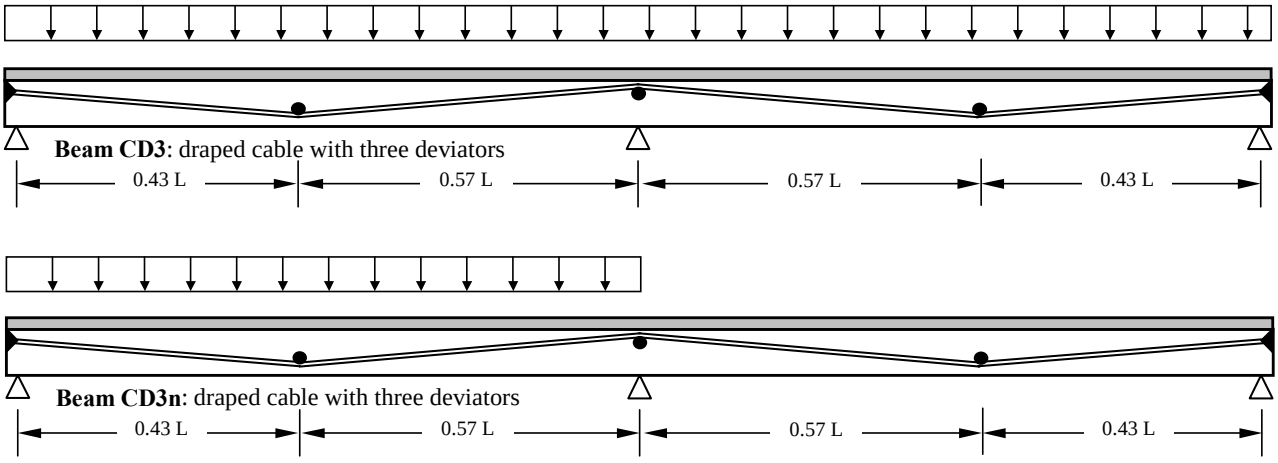

Figure 18. Two-span continuous beams with draped tendon tested

increase in strength is associated to a significant reduction of deflections (Table 3 and Figure 20). The material-nonlinear-only analysis overestimates the peak load level with respect to the geometric nonlinear analysis of 12.9%, and 9.8% for symmetric and non symmetric loading respectively.

As discussed in the previous case of simply supported beams with draped tendons, the tendon forces at the same deflection level are smaller when the moderate rotation analysis is performed (Figure 21) while larger prestressing forces under the same load level are obtained from the geometric nonlinear analysis (Figure 22).

Table 3. Continuous beams tested: loads and mid span deflections

Beam	Moderate rotations analysis				Geometric linear analysis			
	q_{max}	$v(q_{max})$	q_{ult}	v_{ult}	q_{max}	$v(q_{max})$	q_{ult}	v_{ult}
	(kN/m)	(mm)	(kN/m)	(mm)	(kN/m)	(mm)	(kN/m)	(mm)
CNPS	100.59	1350	100.59	1350	100.59	1350	100.59	1350
CNPN	98.41	1382	98.41	1382	98.41	1382	98.41	1382
CD3S	154.70	715	154.60	730	174.75	1015	174.75	1015
CD3N	143.96	610	142.93	765	158.08	1065	158.08	1065

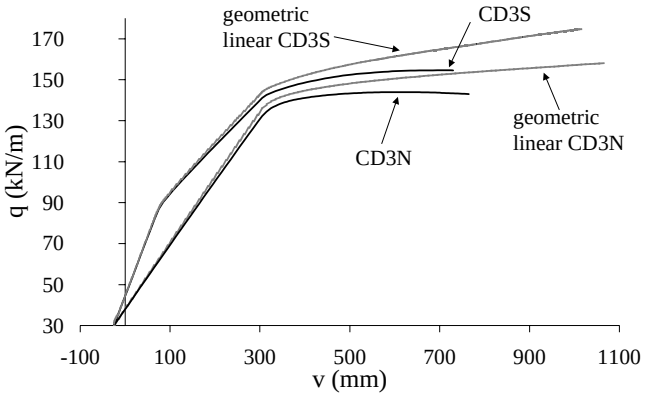

Figure 19. Beams CD3S and CD3N: load – mid span deflection

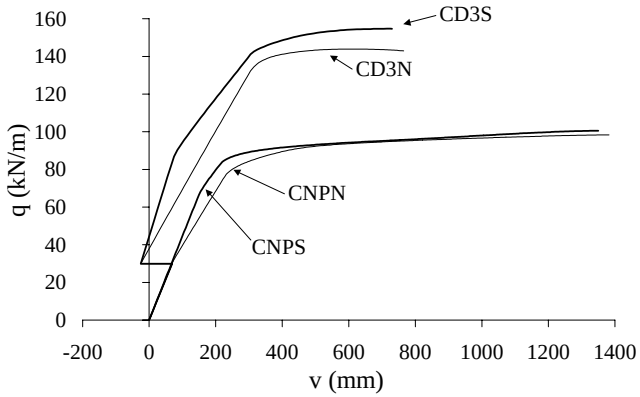

Figure 20. Beams CD3S, CD3N, CNPS, CNPN: load – mid span deflection (moderate rotations analysis)

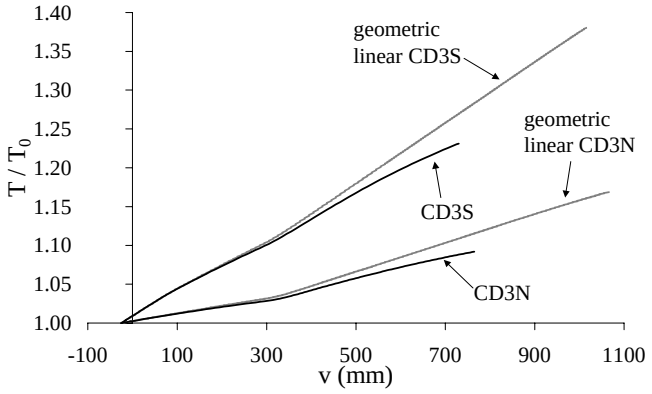

Figure 21. Beams CD3S and CD3N: cable traction – mid span deflection

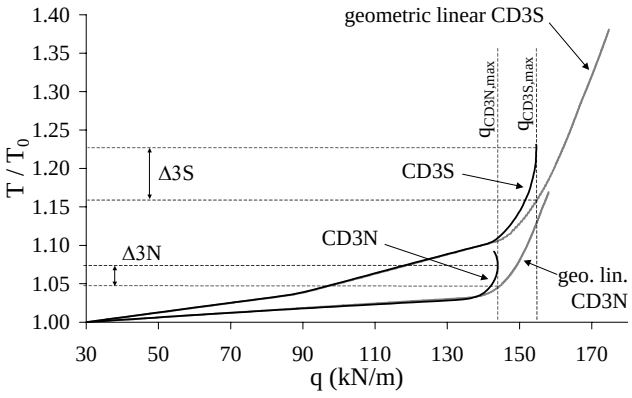

Figure 22. Beams CD3S and CD3N: cable traction – load.

In Figure 23 and in Figure 24 the total bending moment is plotted for the symmetric and non symmetric loading conditions respectively under the corresponding peak load levels (i.e., $q_{CD3S,max}$ for symmetric loading, and $q_{CD3N,max}$ for the non symmetric loading). The bending moment due to prestressing only is also reported (i.e., primary moment computed from the actual tendon eccentricity and traction force without including the secondary moment due to the redundant system of supports). As in the previous cases bending moments computed by the geometric nonlinear analysis are compared to the bending moments from geometric nonlinear analysis under the same load levels.

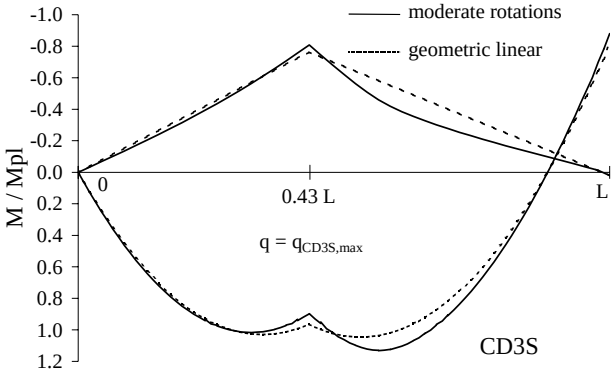

Figure 23. Total bending moment and moment due to prestressing force for beam CD3S

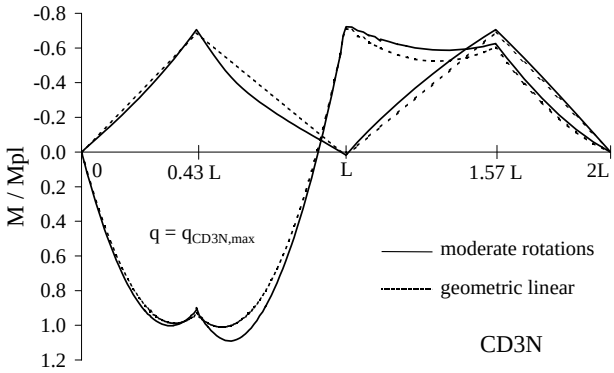

Figure 24. Total bending moment and moment due to prestressing force for beam CD3N

It is observed that at the deviators the total bending moment has a lower value with sign (i.e., smaller absolute value for positive moment and larger absolute value for negative moment) in the geometric nonlinear analysis rather than in the geometric linear analysis. Again the explanation is in the larger prestressing force under the same load. The amount of these bending moment differences are proportional to the difference of the external prestressing force highlighted in Figure 22. In sections sufficiently far from deviators there is an increase or decrease of the bending moment with sign depending on if the span has a downward deflection or un uplift. In fact the cable eccentricity decreases for a downward deflection of the beam while it increases for an uplift. This is clearly shown in two-span beam under non symmetric loading where the first span has a downward deflection and the second span has a upward deflection. The increase of bending moment in the critical section leads to the differences in ultimate load and ductility of the system.

6. CONCLUSIONS

In this work a model for geometric and material nonlinear analysis of beams prestressed with external tendons is illustrated. The formulation was obtained by deducing the beam-tendon model from the finite deformation theory. The hypotheses of small strain and moderate rotations were then assumed, according to the ultimate displacements observed in experimental tests. The weak form of the balance condition was obtained by considering the total Lagrangian formulation and the numerical solution was achieved with a displacement-based finite element formulation. Differently from existing methods starting from the linear theory and then including the eccentricity variation of the cable, the proposed moderate rotation model is based on a nonlinear kinematical theory so that all geometric nonlinearities are included. The actual tendon-beam relative position is consistently considered being the equilibrium imposed in the deformed configuration. In addition the balance conditions reveal that other terms, besides the eccentricity variation, play a rule in the evaluation of the cable force and, consequently, in the beam equilibrium. Specifically the proposed approach considers the coupling between the axial and flexural displacement fields of the beam. As

a consequence a correct evaluation of the vertical displacements due to the large axial forces given by the applied prestressing is included. The axial shortenings of the beam given by the large vertical deflections are considered as well. With regards to the cable the moderate rotation theory leads to a quadratic relationship between tendon strain and beam deformations in which the nonlinear influence of displacements and cable inclination is explicitly shown.

The numerical model implemented was verified by comparison with experimental tests on externally prestressed steel-concrete composite beams. Some numerical applications involving slender simply supported and two-span composite beams post-tensioned with external cables were discussed to illustrate the nonlinear geometric effects and their influence on the ultimate capacity.

Generally the moderate rotation model furnishes higher tendon traction increments with respect to the geometric linear analysis. The reason is in the larger vertical displacements which prevails over the cable traction reduction due to the beam axial shortening. Despite the higher value of the tendon traction, the reduced cable eccentricity leads to a lower ultimate load of the externally prestressed beam. In the numerical applications considered the differences in the ultimate load in cases of practical interest (beams with draped cables) the difference can be up to 15%. These variations increase for slenderer beams making geometric linear analysis unrealistic and unsafe. The numerical examples presented in this paper give a glance at the problem; more numerical studies are necessary for defining the applicability limits of the geometric linear analysis and the proposed model can be conveniently used for this task.

REFERENCES

[1] Szilard, R., “Design of prestressed composite steel structures”, Journal of Structural Division, ASCE, 1959, 85(9), pp.97-124.

[2] Hoadley, P.G., “Behavior of prestressed composite steel beams”, Journal of Structural Division, ASCE, 1963, 89(3), pp.21-34.

[3] Berridge, P.S.A. and Donovan, L.H., “Prestressing restores weakened truss bridge”, Civil Engineering, 1959, 26(9), pp.48-49.

[4] Mancarti, G.D., “Strengthening California steel bridges by prestressing”, Transportation Research Record 950, Second Bridge Conference, Transportation Research Board, 1984, pp.183-187.

[5] Conti, E., Tardy, R. and Virlogeux, M., “Friction losses in some externally prestressed bridges in France”, Proceedings of the Workshop on Behaviour of External Prestressing in Structures, Conti E. and Tardy R. editors, Saint-Rémy-lès-Chevreuse, France, 1993.

[6] Virlogeux, M., “Non-linear analysis of externally prestressed structures”, Proc., XI Symp., Fédération Internationale de la Précontrainte (FIP), Hamburg, Germany, 1990, pp.163-195.

[7] Saadatmanesh, H., Albrecht, P. and Ayyub, B.M., “Analytical study of prestressed composite beams”, Journal of Structural Engineering, ASCE, 1989, 115(9), pp.2364-2381.

[8] Ayyub, B.M., Sohn, Y.G. and Saadatmanesh, H., “Prestressed composite girders under positive moment”, Journal of Structural Engineering, ASCE, 1990, 116(11), pp.2931-2951.

[9] Ayyub, B.M., Albrecht, P. and Saadatmanesh, H., “Prestressed composite girders. II: Analytical study for negative moment”, Journal of Structural Engineering, ASCE, 1992, 118(10), pp.2763-2783.

[10] Dall’Asta, A. and Dezi, L., “Nonlinear behavior of externally prestressed composite beams: analytical model”, Journal of Structural Engineering, ASCE, 1998, 124(5), pp.588-597.

[11] Alkhairi, F.M. and Naaman, A.E., “Analysis of beams prestressed with unbonded internal or external tendons”, Journal of Structural Engineering, ASCE, 1993, 119(9), pp.2680-2700.

[12] Harajli, M., Khairallah, N. and Nassif, H., "Externally prestressed members: evaluation of second-order effects", Journal of Structural Engineering, ASCE, 1999, 125(10), pp.1151-1161.
[13] Ramos, G. and Aparicio, A.C., "Ultimate analysis of monolithic and segmental externally prestressed concrete bridges", Journal of Bridge Engineering, ASCE, 1996, 1(1), pp.10-17.
[14] Ariyawardena, N. and Ghali, A., "Prestressing with unbonded internal or external tendons: analysis and computer model", Journal of Structural Engineering, ASCE, 2002, 128(12), pp.1493-1501.
[15] Naghdi, P.M. and Vongsarnpigoon, A., "Small strain accompanied by moderate rotations", Archive for Rational Mechanics and Analysis, 1982, 80(4), 245-283.
[16] Marzano, S. and De Tommasi, D., "Small strain and moderate rotations", Journal of Elasticity, 1993, 32(1), pp.37-50.
[17] Dall'Asta, A. and Zona, A., "Finite element model for externally prestressed composite beams with deformable connection", Journal of Structural Engineering, ASCE, 2005, 131(5), pp.706-714.
[18] Simo, J.C., "A finite strain beam formulation the three-dimensional dynamic problem. Part 1", Computer Methods in Applied Mechanics and Engineering, 1985, 49(1), pp.55-70.
[19] Simo, J.C. and Vu-Quoc, L., "A three-dimensional finite-strain rod model. Part 2: computational aspects", Computer Methods in Applied Mechanics and Engineering, 1986, 58(1), pp.79-116.
[20] Malvern, L.E., "Introduction to the Mechanics of a Continuous Medium", Prentice-Hall, Inc., Englewood Cliffs, NJ., 1969.
[21] Dall'Asta, A., "On the coupling between three-dimensional bodies and slipping cables", International Journal of Solids Structures, 1996, 33(24), pp.3587-3600.
[22] Dall'Asta, A. and Zona, A., "Slip locking in finite elements for composite beams with deformable shear connection", Finite Elements in Analysis and Design, 2004, 40(13-14), pp.1907-1930.
[23] CEB-FIP, Comité Euro-International du Béton (1988). "Model Code 1990." *CEB Bulletin d'Information*. n. 190, Paris, France.
[24] Bazant, Z.P., Pan, J. and Pijaudier-Cabot, G., "Softening in Reinforced Concrete Beams and Frames", Journal of Structural Engineering, ASCE, 1987, 113(12), pp.2333-2347.
[25] Bruneau, M., Uang, C.M. and Whittaker, A., "Ductile Design of Steel Structures", McGraw Hill., 1998.
[26] Menegotto, M. and Pinto, P.E., "Method of analysis for cyclically loaded reinforced concrete plane frames including changes in geometry and nonelastic behavior of elements under combined normal force and bending", Proceedings, IABSE Symposium on Resistance and Ultimate Deformability of Structures Acted on by Well-Defined Repeated Loads, International Association for Bridge and Structural Engineering, Zurich, 1973, pp.112-123.
[27] Chen, S. and Gu, P., "Load carrying capacity of composite beams prestressed with external tendons under positive moment", Journal of Constructional Steel Research, 2005, 61(4), pp.515-530.